IJCRT.ORG ISSN : 2320-2882

INTERNATIONAL JOURNAL OF CREATIVE RESEARCH THOUGHTS (IJCRT)

An International Open Access, Peer-reviewed, Refereed Journal

Prediction Of Melanoma From Dermoscopic Images Using Deep Learning Based Artificial Intelligence Technique

Ravikiran R, Assistant Professor
Dept of Electronics and Communication
SJC Institute of Technology
Chikballapur, Karnataka, India

Lokepalli Anvitha
Dept of Electronics and Communication
SJC Institute of Technology
Chikballapur, Karnataka, India

Kanchukommla Jayaprakash
Dept of Electronics and Communication
SJC Institute of Technology
Chikballapur, Karnataka, India

Lakshmi G N
Dept of Electronics and Communication
SJC Institute of Technology
Chikballapur, Karnataka, India

***Abstract*—** Skin cancer, among the deadliest cancers, poses a significant threat when not detected and treated promptly. Sun exposure accelerates the proliferation of skin cells, leading to its development. Early detection is crucial to prevent its spread to other parts of the body. This study proposes a computerized technique for skin cancer classification, capitalizing deep convolutional neural networks (CNNs) to enhance diagnostic accuracy and efficiency. The dataset encompasses nine distinct types of skin cancer: seborrheic keratosis, actinic keratosis, benign keratosis, nevus, vascular lesions, basal cell carcinoma, dermatofibroma, melanoma, and squamous cell carcinoma, the aim is to develop a CNN model capable of accurately diagnosing and categorizing skin cancer into these classes. By integrating image processing and deep learning techniques, augmented with various image augmentation strategies, the dataset's diversity is enhanced, thereby improving the model's robustness and generalization capability. The eventual aim is to achieve notable performance metrics for classification tasks adopting the CNN approach. The expected outcomes include a weighted average precision of 0.88, a weighted average recall of 0.74, a weighted average f1-score of 0.80, and an overall accuracy of 90.51%. These metrics serve as benchmarks for evaluating the effectiveness and reliability of the suggested CNN methodology in diagnosing skin cancer.

***Keywords*—** CNN Method, Image processing, Melanoma, Skin cancer, Classification and detection.

I. INTRODUCTION

Skin cancer has materialized as a prevalent global health concern, with both non-melanoma and melanoma skin cancer showing increased incidence over recent decades. One in three cancer cases globally are analogous to skin cancer, according to the World Health Organization (WHO), and one in five Americans will get skin cancer in their lifetime, according to figures from the Skin Cancer Foundation.Regions such as the United States, Canada, and Australia have seen a steady rise in the profusion of individuals affected by skin cancer over the past few centuries. Skin cancer, significantly impact global population health. In 2017, a study revealed that skin cancer contributed to 1.79% of the worldwide disease burden, measured in disability-adjusted life years. Approximately 7% of new cancer cases globally are attributed to skin cancer, with associated costs exceeding $8 billion for the US Medicare program in 2011.

Clinical evidence suggests variations in skin cancer outcomes based on race: individuals with dark hued tones are generally 20 to 30 percent less susceptible to melanoma compared with lighter hued tones. However, mortality risks for certain types of melanoma may vary, with some melanoma types showing higher or lower ephemerality rates among divergent racial groups. Skin cancer frequency rates fluctuate across countries, as proclaimed by the World Cancer Research Foundation. Latterly, Convolutional Neural Networks (CNNs) have gained widespread use for skin cancer classification. These models have often surpassed the diagnostic accuracy of even experienced healthcare professionals. Techniques such as transfer learning, which involves imposing on large datasets, have further improved CNN performance. Well-known CNN designs, such as VGG-16 and VGG-19, with 16 and 19 convolutional layers, respectively, have allowed to catalogue skin cancer. These pre-trained networks are capable of

recognizing a vast range of objects, from conventional items like keyboards and mice to various creatures, across 1000 object categories. With input data resolution typically set at 224-by-224 pixels, these networks have accumulated rich feature representations from extensive image datasets.

II. DATA PRE-PROCESSING

In regulation to boost the persuasiveness of suspected sickness diagnoses, we shall use simulation techniques to draw attention to significant issues with visual identification.

A. Dataset

The dataset, sourced from Kaggle.com, comprises 25,780 images depicting benign skin lesions and malignant skin lesions. Each image is categorized based on descriptions prevalent by the International Skin Imaging Collaboration (ISIC), with subgroups including, dermatofibroma, seborrheic keratosis, squamous cell carcinoma, basal cell carcinoma, melanoma, nevus, vascular lesion and actinic keratosis. The dataset is publicly available, accompanied by metadata that facilitates documentation for each image, allowing for comparisons and analysis. To ensure consistency, all images have been modified to 224 x 224 pixels as part of the data preprocessing stage. Furthermore, the dataset has been prorated into three subsets: training, validation, and testing, with respective sizes of 19,537, 2,167, and 3,799 samples. This division allows for robust model training, validation, and evaluation processes.

B. Data Augmentation

Making the most of the amount of data is beneficial as well. The data augmentation strategy is crucial for correctly training a CNN model. This method keeps the original consistency of the input and output data while avoiding distortion. Furthermore, this procedure is carried out precisely while the model is being trained, allowing for the overfitting issue to be resolved and advancing the model's output. In order to choose values from different sizes, we have multiple options for image augmentation, including rotation range, shear range zooming, and horizontal flip. In order to aggrandize the model's utility during training, each option has the capacity to represent images in a multitude of ways and to supply crucial features.

Fig. 1. Images from Dataset

III. METHODOLOGY

Convolutional Neural Networks (CNNs) draw revelation from biological systems, particularly the visual cortex's neuron arrangement. CNNs constitute three major layers: Convolutional layer, Pooling layer, and Fully-Connected layers. The key components of a CNN system include feature extraction, detection, and classification. The process starts with a convolutional layer, followed by activation and max-pooling layers to extract features concurrently. These characters are then acknowledged through parallel layers at the functional level. Next, the flattened features are fed into Multi-Layer Perceptron's (MLPs) with two levels, adjusting the number of neurons in each layer to prevent overfitting. The final classification is performed by a layer containing the SoftMax function. Class activation maps are engendered in these layers, serving as a classification guide linked to the last convolutional layer. The workflow is divided into two sections: extraction and classification/detection. The first section focuses on feature extraction, while the latter deals with image classification and detection. This division enhances the adaptability and incisiveness of the CNN model in processing and interpreting visual data.

A. Feature Extraction Phase

It is crucial to use filters of different sizes and assess a range of performance parameters in order to set up an efficient network architecture in each convolution layer. In the initial phase, our CNN model comprises five dilated convolutionary units, denoted as CBr = iconv (n = 64,128,256,512,512), which are alternatively max-pooled. Our model incorporates dilated convolution, in which the input picture feeds into two simultaneous CBr=iConv blocks with just the dilation amount (di = 1, 2, 3,..., N) separating them. By processing data at a higher resolution and collecting finer visual details, a dilation rate larger than 1 improves the convolution layer's performance. The receptive field, which denotes the region of the image influenced by the filter without altering its magnitude, remains constant across different dilation rates, resulting in the markdown of pixels in each input corresponding to the dilation rate (di - 1). In simpler terms, when the dilation rate is 1, it's akin to a standard convolution operation. However, for a dilation rate of 2, in a two-dimensional input image, every other pixel is skipped. The relationship between the dilation rate (di) and the receptive field (rf) can be understood by considering the impact of di on rf given a kernel size (ks). If the kernel size is ks and it undergoes dilation by di, the expression for the receptive field can be represented as Equation no. 1,

rf = di(k1) + 1 (1)

The amount of output O is shown by Equation No. 2 if the input is i× i with a dilation factor of di, padding of pd, and stride of st, respectively, and the output is O.

O = i + 2pdrf st + 1 (2)

At different scales, important features in the observing region are reported using two receptive fields of differing sizes. The presently introduced prototype consists of three CBr=iconv blocks, the latter two of which contain four convolution layers and an activation layer, and the first two of which have two convolution layers each. Furthermore, every block in this group has a distinct filter (3 × 3), with stride and dilation rates of 1 and di, respectively. Filters Fs R1→n can be used to define the convolution layer; the equation is provided below.

Fs = fj→j 1 fj→j 2 ...fj→j n=x (3)

here, j × j is filter size. The suggested convolution network will produce Y mf →mf l feature maps from the inputs if layer l's dilation rate is di and mf x mf is designated as the input feature map. which the following equation can be used to calculate:

Y o→o l = Y mf →mf l1, di=k →l f + lb (4)

here, lb is the bias of the layer, and lf is filter. Following the convolution layer, the generated features undergo activation through a chosen nonlinear layer, typically denoted as "a", which is commonly merged into CNNs. Because of a number of advantages, including the capacity to promote gradient propagation and lower the likelihood of gradient vanishing during the early phases of CNN computation, ReLU (Rectified Linear Unit) is frequently chosen for this function. The activation function works element-by-element on the input feature map, producing an output map that is the same size as the input. This is important to note. In our devised scheme, a block of CBr = iconv, paired with a max-pooling layer, is incrementally repeated five times in succession. Max-pooling serves as an effective method for down sampling the feature maps, with a 2x2 filter size and a stride of 2 being utilized at each layer. This strategy efficiently reduces the dimensionality of the feature maps, enhancing the performance of subsequent computational steps. Overlapping max-pooling windows were not employed, as their benefits were not deemed significant compared to non-overlapping windows. Low-level features are produced by a ReLU activation function unit after the last convolution layer, which consists of 512 filters with a j x j kernel size and runs at a dilation rate of 1. The convolution layer's parallel branches yield features that are concatenated. By examining the link between dilated convolution blocks, the final convolution layer can identify higher classification features credits to the concatenation of unique characteristics from various layers, which is captured by each branch. Subsequently, in the flattened layer, the model transforms the feature maps into a one-dimensional feature vector, essential for the classification task. Ultimately, this one-dimensional feature vector is employed by the classification phase to carry out the classification task, which will be covered, more particular in the following section. Two neural layers are used in the classification phase. A two-layer MLP, sometimes referred to as a completely connected (FC) layer, fed the output from the flattened level during that stage in order to accomplish the classification process. In addition, a dropout layer is linked after each FC layer. To reduce overfitting, these dropout layers will randomly remove some FC layer weights amid the training process. The dropout range, which spans from 0% to 100%, determines the quantity of weight drops selected at random. We have selected the dropout range of 0.5 for analytical reasons. In addition, the sizes of the two fully connected layers are 4096 & 4096 FC, respectively. The SoftMax activation function has been applied after the fully connected layer to help separate skin cancer photos, such as those with actinic keratosis, benign keratosis, basal cell carcinoma, dermatofibroma, melanoma, seborrheic keratosis, vascular lesions, squamous cell carcinoma, and nevus.

IV. FLOW CHART OF MODEL

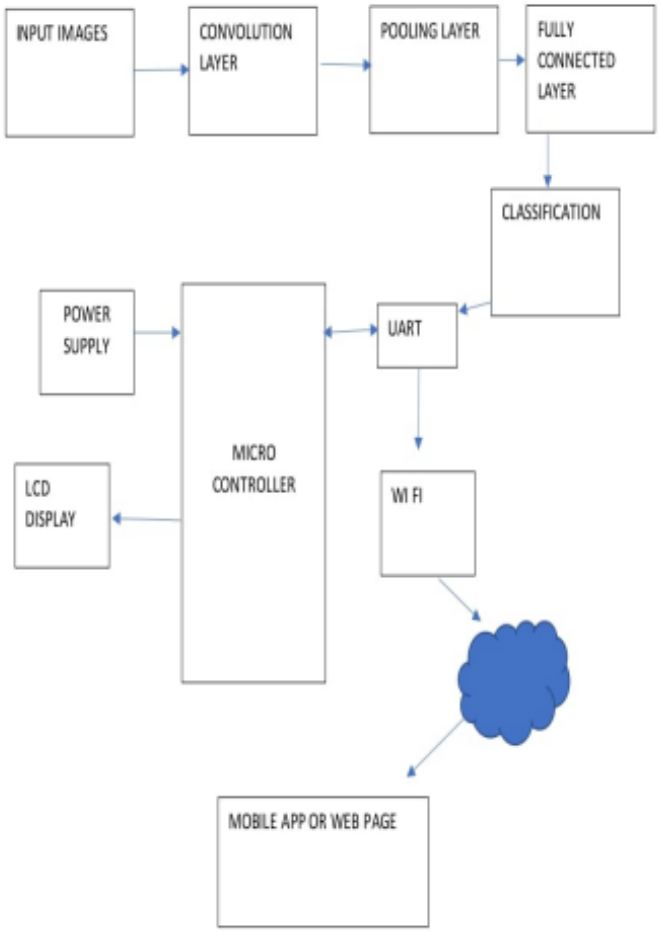

Fig. 2. Flowchart

V. ADVANTAGES

- Deep learning models can encounter melanoma at an early stage, increasing the chances of outstanding treatment and reducing mortality rates.
- AI systems can analyses images quickly, allowing for faster diagnosis and reducing patient risk.
- AI can process a large number of images, making it suitable for population-level screening and early detection efforts.
- Early detection can bring about cost savings by avoiding the need for extensive treatments at advanced stages of melanoma.
- AI can also be habituated to educate patients about melanoma risks and promote regular skin checks.

VI. APPLICATIONS

- *Digital Photographs:* CNN's have been used to classify digital photographs of skin lesions as malignant.

- *Mobile apps:* There have been considerable mobile apps developed that CNNs to analyze images of skin lesion and provide a prediction of whether they are malignant and non-malignant.

VII. RESULT

A Convolutional Neural Network (CNN) approach is employed for diagnosing skin cancer and categorizing it into various groups, leveraging image recognition and deep learning algorithms. Initially, dermoscopic images of skin cancer is processed by removing noise and adjusting picture resolution. Different image augmentation techniques are adapted to increase the diversity of the dataset. Subsequently, Transfer Learning is utilized to enhance image recognition accuracy further. The CNN model achieves promising performance metrics with a weighted average Precision of 0.88, weighted average Recall of 0.74, and a weighted F1-score of 0.80. These metrics indicate the model's capacity to meticulously classify skin cancer cases across different categories. Furthermore, the Transfer Learning approach, specifically utilizing the ResNet model, achieves an impressive accuracy rate of 90.51%. Transfer Learning allows leveraging pre-trained models trained on vast datasets, thereby enhancing the model's capacity to generalize and achieve high accuracy even with bounded training data. Overall, this method demonstrates the efficacy of CNNs coupled with Transfer Learning for accurate and efficient diagnosis of skin cancer, offering promising results in words of accuracy and performance metrics.

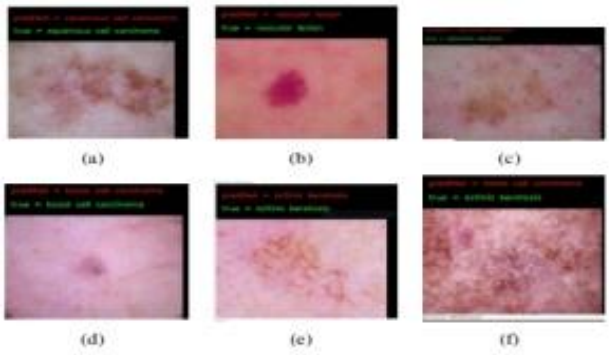

Fig. 3. Detection result Of Model

VIII. CONCLUSION

This paper presents a powerful model for detecting and classifying melanoma, a type of skin cancer. Our model leverages cutting-edge technologies such as image processing, image augmentation, Internet of Things (IoT), artificial intelligence, and deep learning techniques to deliver accurate and reliable results. It scans input images and identifies them based on nine different skin cancer classifications with utmost precision. The outcomes are then uploaded to the cloud or other storage using WIFI modules and delivered directly to the patient's smartphone. Our model is capable of detecting cancer at an early stage, which significantly increases the contingent of successful treatment and cure. We strongly emphasize the consequence of initial stage detection and classification of skin cancer.

REFERENCES

[1] M. A. Kassem, K. M. Hosny, and M. M. Fouad, ‘‘Skin lesions classification into eight classes for ISIC 2019 using deep convolutional neural network and transfer learning,’’ IEEE Access, vol. 8, pp. 114822–114832, (2020).

[2] Natasha nigar , Muhammad umar, Muhammad kashif shahzad, Shahid islam and douhadji abalo.”A Deep Learning Approach Based on Explainable Artificial Intelligence for Skin Lesion Classification”.(2022)

[3] S. H. Kassani and P. H. Kassani, ‘‘A comparative study of deep learning architectures on melanoma detection,’’ Tissue Cell, vol. 58, pp. 76–83, (Jun. 2021).

[4] J. A. A. Salido and C. Ruiz, ‘‘Using deep learning for melanoma detection in dermoscopy images,’’ Int. J. Mach. Learn. Comput., vol. 8, no. 1, pp. 61–68, Feb. 2019.

[5] H. M. Ünver and E. Ayan, ‘‘Skin lesion segmentation in dermoscopic images with combination of Yolo and GrabCut algorithm,’’ Diagnostics, vol. 9, no. 3, p. 72, Jul. (2022).

[6] M. R. Zafar and N. Khan, ‘‘Deterministic local interpretable modelagnostic explanations for stable explainability,’’ Mach. Learn. Knowl. Extraction, vol. 3, no. 3, pp. 525–541, Jun. (2021).

[7] S. A. Ajagbe, K. A. Amuda, M. A. Oladipupo, F. A. Oluwaseyi, and K. I. Okesola, ‘‘Multi-classification of Alzheimer disease on magnetic resonance images (MRI) using deep convolutional neural network (DCNN) approaches,’’ Int. J. Adv. Comput. Res., vol. 11, no. 53, p. 51, (2021).

[8] H. Zunair and A. B. Hamza, ‘‘Melanoma detection using adversarial training and deep transfer learning,’’ Phys. Med. Biol., vol. 65, no. 13, (July 2020).

[9] B. H. M. van der Velden, H. J. Kuijf, K. G. A. Gilhuijs, and M. A. Viergever, ‘‘Explainable artificial intelligence (XAI) in deep learning-based medical image analysis,’’ Med. Image Anal., vol. 79, (Jul. 2022), Art. no. 102470.

[10] Y. Xie, J. Zhang, Y. Xia, and C. Shen, ‘‘A mutual bootstrapping model for automated skin lesion segmentation and classification,’’ IEEE Trans. Med. Imag., vol. 39, no. 7, pp. 2482–2493, (Dec. 2020)

[11] B. Ankad, P. Sakhare, and M. Prabhu, ‘‘Dermoscopy of non-melanocytic and pink tumors in Brown skin: A descriptive study,’’ Indian J. Dermatopathol. Diagnostic Dermatol., vol. 4, no. 2, p. 41, (2020).

[12] T. J. Brinker, A. Hekler, A. H. Enk, J. Klode, A. Hauschild, C. Berking, B. Schilling, S. Haferkamp, D. Schadendorf, T. Holland-Letz et al., “Deep learning outperformed 136 of 157 dermatologists in a headto-head dermoscopic melanoma image classification task,” European Journal of Cancer, vol. 113, pp. 47–54, 2019.

[13] L. Yu, H. Chen, Q. Dou, J. Qin, and P.-A. Heng, “Automated melanoma recognition in dermoscopy images via very deep residual networks,” IEEE transactions on medical imaging, vol. 36, no. 4, pp. 994–1004, 2016.

[14] Esteva, B. Kuprel, R. A. Novoa, J. Ko, S. M. Swetter, H. M. Blau, and S. Thrun, “Dermatologist-level classification of skin cancer with deep neural networks,” nature, vol. 542, no. 7639, pp. 115–118, 2017.

[15] H. A. Haenssle, C. Fink, R. Schneiderbauer, F. Toberer, T. Buhl, A. Blum, A. Kalloo, A. B. H. Hassen, L. Thomas, A. Enk et al., “Man against machine: diagnostic performance of a deep learning convolutional neural network for dermoscopic melanoma recognition in comparison to 58 dermatologists,” Annals of Oncology, vol. 29, no. 8, pp. 1836–1842, 2018.

[16] N. C. Codella, Q.-B. Nguyen, S. Pankanti, D. A. Gutman, B. Helba, A. C. Halpern, and J. R. Smith, "Deep learning ensembles for melanoma recognition in dermoscopy images," IBM Journal of Research and Development, vol. 61, no. 4/5, pp. 5–1, 2017.

[17] M. Attia, M. Hossny, S. Nahavandi, and A. Yazdabadi, "Skin melanoma segmentation using recurrent and convolutional neural networks," in 2017 IEEE 14th International Symposium on Biomedical Imaging (ISBI 2017). IEEE, 2017, pp. 292–296.

[18] N. Nida, A. Irtaza, A. Javed, M. H. Yousaf, and M. T. Mahmood, "Melanoma lesion detection and segmentation using deep region based convolutional neural network and fuzzy c-means clustering," International journal of medical informatics, vol. 124, pp. 37–48, 2019.

[19] N. C. Codella, D. Gutman, M. E. Celebi, B. Helba, M. A. Marchetti, S. W. Dusza, A. Kalloo, K. Liopyris, N. Mishra, H. Kittler et al., "Skin lesion analysis toward melanoma detection: A challenge at the 2017 international symposium on biomedical imaging (isbi), hosted by the international skin imaging collaboration (isic)," in 2018 IEEE 15th International Symposium on Biomedical Imaging (ISBI 2018). IEEE, 2018, pp. 168–172